How Gravity and Joint Scaling Affect Dynamic Response

S. T. Hsu,* J. H. Griffin,* and J. Bielak†
Carnegie Mellon University, Pittsburgh, Pennsylvania

If a scale model of a space structure is ground tested to establish dynamic characteristics of a full-scale space structure, two factors need to be taken into consideration: the joint tolerances may not be scaled, and joint preloads (from gravity) may be present. In some situations, these differences may significantly affect dynamic response so that the model is not representative of the structure in space. In this study, joint effects are investigated by considering the response of a single-degree-of-freedom system that is restrained by a joint linkage. The joint is characterized by its initial stiffness, the load at which it slips, its hardening rate, and the distance it can slip (joint "slop" or gap). The steady-state response of the system is calculated using a harmonic balance approach. It is found that the system response is multivalued for certain ranges of gap dimensions. When this is the case, small changes in system properties can lead to large differences in dynamic response and make it difficult to obtain meaningful results directly from model testing.

Introduction

MANY engineering structures are subjected to motions in which limited slip can occur between members. This is frequently the case for bolted and riveted structures and can also occur in joints found in space applications. Truss structures designed for space often are constructed with joints that can rotate and lock into place. This allows the structure to collapse into a compact package that is easily transported to space and then expanded. Typically, this type of joint mechanism is subject to limited slip behavior because of "slop" due to machining tolerances. In addition, joint slip is usually constrained by friction forces within the mechanism. This means that the joint's motion is controlled by friction until it reaches the end of the free play and then it is constrained elastically. This type of nonlinear behavior can have a strong influence on system response. In particular, because of the limited slip or the "gap" aspect of the joint behavior, scaled models of the jointed structure may not respond dynamically in the same manner as the full-scale structure in space. This may be the case for two reasons.

The first reason that a scaled model of a structure may not have the same dynamic response is that tolerances in the joints are not scaled. Typically, engineers wish to have joints that behave linearly. Consequently, when designing the full-scale joint they stipulate tolerances as small as possible to reduce slop and the associated nonlinear behavior. When scale models of the joint are developed for testing, the same absolute tolerances are stipulated since they cannot be reduced further. As a result, the free play in the scaled joints is, on average, significantly greater than in full-scale joints; consequently, the model structure will exhibit stronger nonlinear behavior.

A second reason that a scaled model of a structure may behave differently is that it may be tested under gravitational loading that does not occur in space. Although there are laboratory procedures for supporting two-dimensional structures (i.e., structures that have modes in which the motions lie in a plane) in such a way as to negate gravitational effects, they are not readily applicable to more complex, three-dimensional structures. As a result, it is not possible, in general, to eliminate gravitationally induced preloads in the joint. The preload introduces a static displacement in the joint that tends to eliminate the free play in one direction. For example, the joint may behave elastically in the direction of the applied preload and slip only when motion occurs in the opposing direction (in contrast to a joint without any static loads that slips in both directions). From a dynamics point of view, a joint with preloads tends to be effectively stiffer and contributes less damping to the system. A goal of the current research is to gain a better understanding of this effect.

This research considers the dynamic response of the lumped-parameter system depicted in Fig. 1a. The friction element can slide once the magnitude of the force reaches μN. The response of the nonlinear element that represents the joint is indicated in Fig. 1b. Note that when the joint is stuck, it has a stiffness of $k_1 + k_2$, whereas when it slips the force continues to increase, but at a lower rate. (Frequently, a lower but nonzero rate of increase is apparent in actual joint data and may be associated with variable normal load effects. The assumption that the normal load varies linearly with the magnitude of the joint's displacement is used by Hertz and Crawley.[1]) In this model, joint slip is limited by stops and, as a result, the joint hardens elastically beyond a certain point. We confine our research to the study of joints with these main attributes. (An additional joint attribute that could be considered is microslip. Microslip can play an important role in joint response when the excitation is small or when the normal load is hight. For example, see Refs. 2-4.)

The remaining part of the space structure is represented by the mass, spring, and dashpot in Fig. 1a that lies in series with

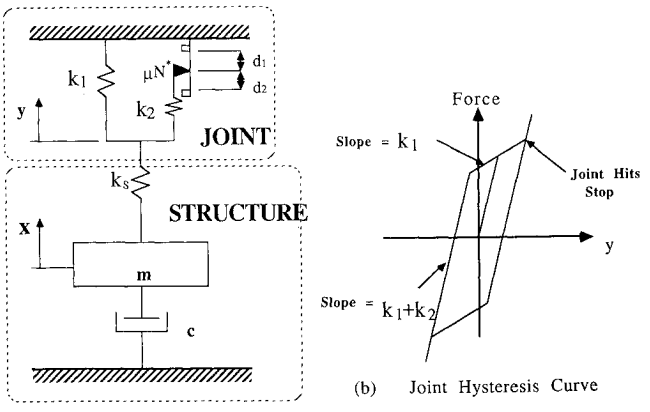

(a) Simple Jointed Structure (b) Joint Hysteresis Curve

Fig. 1 System model.

Received Sept. 24, 1987; revision received Sept. 15, 1988. Copyright © 1989 American Institute of Aeronautics and Astronautics, Inc. All rights reserved.

*Department of Mechanical Engineering.
†Department of Civil Engineering.

the joint and may be thought of as a single-mode approximation of the response of that substructure. It can be shown that the system of Fig. 1 can be reduced to that depicted in Fig. 2 provided that the constants k, k_d, μN, and δ_i are selected as

$$k = \frac{k_1 k_s}{k_1 + k_s}, \qquad k_d = \frac{k_s^2 k_2}{(k_1 + k_s)(k_1 + k_2 + k_s)}$$

$$\mu N = \frac{\mu N^* k_s}{k_1 + k_s}, \qquad \delta_i = d_i \frac{(k_s + k_1)}{k_s} \tag{1}$$

The system is subjected to a sinusoidal excitation and a static preload in order to simulate the effect of gravity. This system was chosen for examination because it is the simplest system that exhibits the characteristics of interest, and yet, in a modal sense, has implications to a broad class of systems. This paper concentrates on establishing the steady-state response of this system and on determining under what conditions it exhibits multiple solutions.

The presence of multiple solutions is, in general, undesirable since the dynamic response of the system can change abruptly for small variations in the input parameters. When multiple steady-state solutions exist, the long-time solution that the system achieves depends on the initial state of the system. Consequently, when conditions exist under which multiple solutions can occur, the transient response, as well as the steady-state response of the system, can be extremely sensitive to perturbations in either the system parameters or the initial conditions. In addition, the presence of multiple solutions can lead to vertical jumps in the frequency response, and the jump can change depending on whether the excitation frequency is increasing or decreasing. This type of instability and its relation to vertical jumps is discussed by Den Hartog.[5] Consequently, this situation can lead to difficulties in testing and in analysis and should be avoided.

A general discussion of the procedures and difficulties associated with the testing of space structures is given by Hanks and Pinson.[6] A procedure for testing joints and identifying nonlinear mechanisms is discussed by Crawley and Aubert.[7] Research on the response of systems with friction constraints was summarized in 1980 by Plunkett[8] and more recently in a series of reviews by Jones[9] and Beards.[10] The dynamic response of lumped mass/spring systems with friction constraints has received considerable attention in the literature. Relevant examples of these include Den Hartog's analysis of a single-degree-of-freedom system in which the friction element is rigid/perfectly plastic,[11] Caughey's analysis of an elastic/perfectly plastic element,[12] and Iwan's analysis of a friction element with gaps.[13] Den Hartog and Caughey's results show that frictionally damped systems can have unbounded response near resonance but that, in general, the response of these systems tends to be relatively smooth and single valued. Iwan shows that the addition of stops can lead to multiple solutions. The system studied in this paper has viscous damping and, consequently, does not exhibit unbounded response. It differs from the system considered by Iwan in that it has the additional spring element with stiffness k (Fig. 2) and considers the effect of static preload.

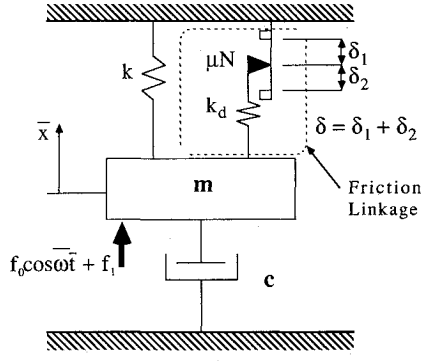

Fig. 2 Reduced system.

II. Analysis

In this section, we describe our approach for calculating the response of the system under consideration. In Sec. II.A, the governing equation for the system is described. Its normalized form is given to provide a basis for parametric studies. The approximate method is introduced in Sec. II.B, and the equations for calculating the frequency response are derived. Section II.C presents the procedure for obtaining resonant response, whereas in Sec. II.D we show how certain limiting frequencies and amplitudes are obtained.

A. Formulation of Governing Equations

The equation of motion for the system shown in Fig. 2, which also represents the response of the original model (Fig. 1), is

$$m\frac{d^2(\bar{x})}{d\bar{t}^2} + c\frac{d\bar{x}}{d\bar{t}} + k\bar{x} = f_o \cos\overline{\omega t} + f_1 - f_n \tag{2}$$

where f_1 is the static load and f_n the nonlinear force associated with the friction part of the linkage in Fig. 2.

We use a Coulomb model of friction, i.e, the friction element will slide once the magnitude of the force f_n equals N multiplied by μ, the friction coefficient of the materials in contact. The force f_n is a function of the mass displacement x. When $|x| \le \mu N/k_d$, where k_d is the stiffness of the friction element, the system is linear. When $|x| > \mu N/k_d$, and the stop distances δ_1 and δ_2 are sufficiently large, f_n has elastoplastic behavior. When the stop distances δ_1 and δ_2 are not sufficiently large, the system experiences a sudden hardening phenomenon.

To render a basis for the parameteric study, Eq. (1) can be converted into a nondimensional form:

$$\frac{d^2x}{dt^2} + \zeta\frac{dx}{dt} + x = \cos\omega t + \lambda_1 - \lambda_2 F_n \tag{3}$$

where

$$x = \bar{x}/x_o, \qquad t = \bar{t}/t_o, \qquad \omega = \overline{\omega t_o}, \qquad \zeta = c/\sqrt{mk}$$

$$\lambda_1 = f_1/f_o, \qquad \lambda_2 = \mu N/f_o, \qquad F_n = f_n/\mu N$$

$$x_o = f_o/k, \qquad t_o = \sqrt{m/k}$$

One purpose of this study is to understand the steady-state response of the system shown in Fig. 1. Although this task can be accomplished by solving Eq. (3) numerically for a sufficiently long period of time, such an approach is inefficient and computationally expensive. Therefore, an alternate, more efficient approximate method is developed. The direct, long-time solution then is used only to verify the accuracy of the analytical results in certain representative cases.

B. Approximate Method

One of the most popular methods for approximating the frequency response of nonlinear systems is known as the harmonic balance method in the vibration literature, e.g., Ref. 14, and as the describing function approach in the control literature, e.g., Ref. 15. Other methods that are used are known as the equivalent energy balance method, equivalent linearization, the method of slowly varying parameters, as well as various perturbation methods. Iwan[16] shows that if these methods are employed correctly then, to first order, they all yield the same steay-state solution when applied to a frictionally damped system.

The harmonic balance (HB) method will be used here to establish an approximate steady-state solution. The HB

method is based on the observation that if the excitation is periodic, then the response of the system is probably also periodic and of the same period as the excitation. [This is not always the case. In some instances, the response can have a period that is an integer multiple of the excitation or is even chaotic in nature. A number of numerical simulations using time integration were conducted that tracked the transient response in order to check the response of this system (see Figs. 3-6), and in every case the period of the response was the same as the period of the excitation.] Therefore, the displacement x can be expanded in a Fourier series. It is assumed that only the lowest frequency terms are important and x is approximated as

$$x = A\cos\theta + B \tag{4}$$

where $\theta = \omega t - \psi$. Note that the offset term B is included to compensate for the shift due to the static load λ_1. (An offset term was also included in the harmonic balance analysis of a frictionally damped system[17] and is required when either the loading or constraints are not symmetric.)

Consistent with the approximation for x, it is assumed that

$$F_n = F_b + F_c\cos\theta + F_s\sin\theta \tag{5}$$

where F_b, F_c, and F_s, the usual Fourier coefficients, are given in Ref. 18. They are omitted here for conciseness since, for the system under study, separate expressions for the coefficients must be established for the different ranges of response, i.e., no slip, slip but no contact with the stops, contact with one stop, etc.

To obtain the approximate solution, Eqs. (4) and (5) are substituted into Eq. (3). After equating the linearly independent terms, the phase shift ψ is eliminated by using the relation $\sin^2\psi + \cos^2\psi = 1$. Then the following two nonlinear algebraic equations are obtained:

$$g_1(A,B,\omega) \equiv B + F_b - \lambda_1 = 0 \tag{6}$$

$$g_2(A,B,\omega) \equiv [(1-\omega^2)A + F_c]^2 + [\omega\zeta A - F_s]^2 - 1 = 0 \tag{7}$$

Equations (6) and (7) are solved iteratively to determine the frequency response of the vibratory amplitude A and the permanent offset B.

C. Calculation of Resonant Response

By holding the system parameters and the magnitude of the excitation constant, the resonant vibratory amplitude is defined as values satisfying the constraint

$$\frac{\partial A}{\partial \omega} = 0 \qquad \text{at } \omega = \omega_m \tag{8}$$

where ω_m will be referred to as the "resonant frequency." If we can apply this constraint together with Eqs. (6) and (7), we should be able to calculate the system's maximum response without having to perform a frequency search.

Equation (8) is a difficult constraint to use directly. A more convenient and equivalent constraint is derived as follows. First, it is observed that A and B are both functions of ω. Consequently, g_1 and g_2 are only functions of ω, and from Eqs. (6) and (7)

$$\frac{dg_1}{d\omega} = \frac{\partial g_1}{\partial A}\frac{\partial A}{\partial \omega} + \frac{\partial g_1}{\partial B}\frac{\partial B}{\partial \omega} + \frac{\partial g_1}{\partial \omega} = 0 \tag{9}$$

$$\frac{dg_2}{d\omega} = \frac{\partial g_2}{\partial A}\frac{\partial A}{\partial \omega} + \frac{\partial g_2}{\partial B}\frac{\partial B}{\partial \omega} + \frac{\partial g_2}{\partial \omega} = 0 \tag{10}$$

From Eq. (6), we know that $\partial g_1/\partial\omega = 0$; thus, Eqs. (8) and (9) imply that at resonance

$$\frac{\partial g_1}{\partial B}\frac{\partial B}{\partial \omega} = 0 \tag{11}$$

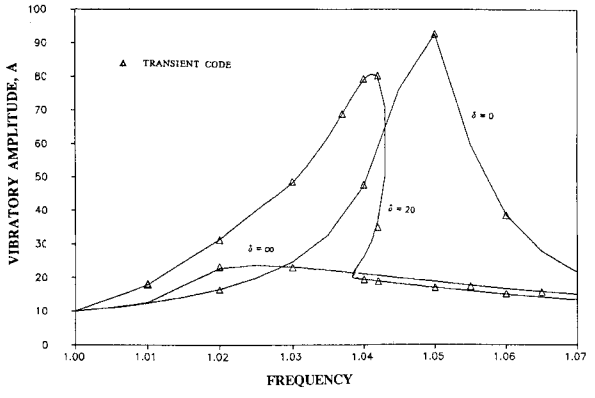

Fig. 3 Vibratory amplitude vs frequency with varied gap length.

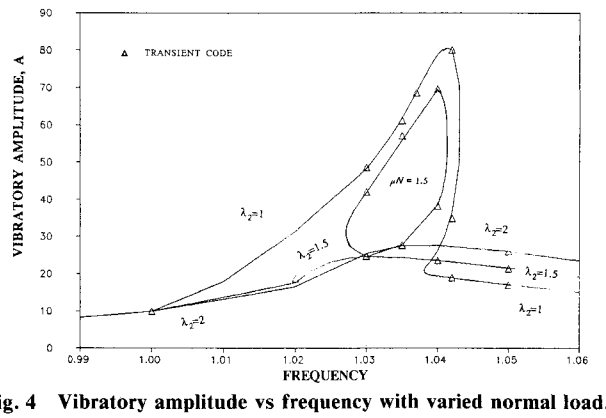

Fig. 4 Vibratory amplitude vs frequency with varied normal load.

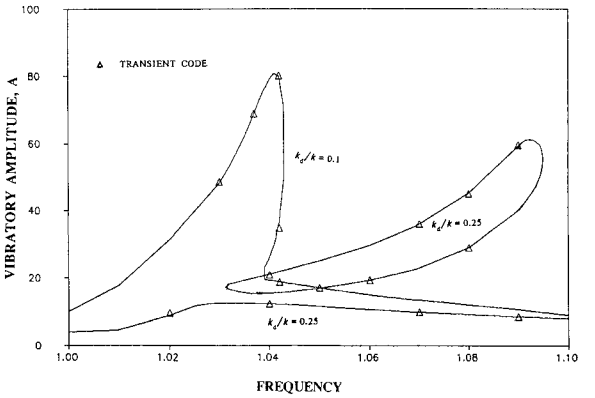

Fig. 5 Vibratory amplitude vs frequency with varied stiffness.

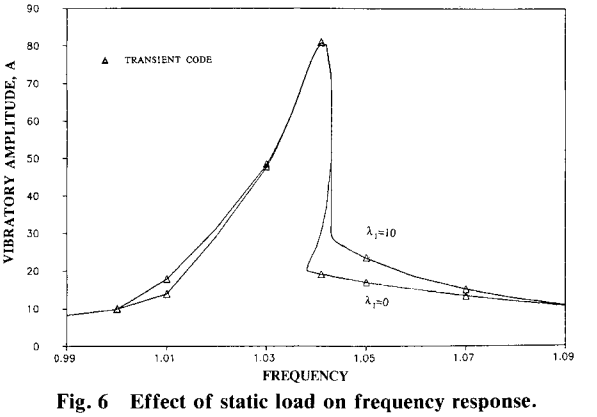

Fig. 6 Effect of static load on frequency response.

and since from Eq. (6) $\partial g_1/\partial B = 1$, we have

$$\frac{\partial B}{\partial \omega} = 0 \qquad \text{at } \omega = \omega_m \tag{12}$$

Consequently, Eqs. (7), (8), (10), and (12) imply

$$\frac{\partial g_2}{\partial \omega} = \{\zeta(\omega\zeta A - F_s) - 2\omega[(1-\omega^2)A + F_c]\}(2A) = 0$$

$$\text{at } \omega = \omega_m \tag{13}$$

Thus, the three equations that determine the resonant values A and B at the corresponding resonant frequency of excitation are

$$g_1(A_m, B_m, \omega_m) = 0 \tag{14a}$$

$$g_2(A_m, B_m, \omega_m) = 0 \tag{14b}$$

$$\frac{\partial g_2}{\partial \omega}(A_m, B_m, \omega_m) = 0 \tag{14c}$$

In practice, Eqs. (14) are solved more conveniently in the following manner. Adding Eq. (7) to Eq. (13), after multiplying the others by ω_m, we have

$$F\omega_m^4 + G\omega_m^2 + H = 0 \tag{15}$$

where

$$F = 5A_m^2 \tag{16a}$$

$$G = 3[(\zeta^2 - 2)A_m^2 - 2A_mF_c] \tag{16b}$$

$$H = A_m^2 + F_c^2 + 2A_mF_c + F_s^2 - 1 \tag{16c}$$

Also, by substituting Eq. (13) into Eq. (7), we have

$$(\omega_m\zeta A_m - F_s)^2[1 + (\zeta/2\omega_m)^2] = 1 \tag{17}$$

Therefore, from Eqs. (6), (17), into (15), the following iterative equations for calculating the resonant response can be obtained:

$$B_m = \lambda_1 - F_b \tag{18a}$$

$$A_m = [F_s + 1/\sqrt{1 + (\zeta/2\omega_m)^2}]/\zeta\omega_m \tag{18b}$$

$$\omega_m = \left\{\left(\frac{1}{2F}\right)\left(-G + \sqrt{G^2 - 4FH}\right)\right\}^{1/2} \tag{18c}$$

To solve Eqs. (18), group values of A_m, B_m, and ω_m are first initialized to calculate the Fourier coefficients F_b, F_s, and F_c. Iterations are then made using Eqs. (18) until A_m, B_m, and ω_m converge.

D. Calculation of Vertical Tangencies

As will be seen, points of vertical tangency can be used to establish over what range of frequencies multiple solutions can occur. When the system parameters are constant, vertical tangency occurs when

$$\frac{\partial A}{\partial \omega} \to \infty \text{ or } \frac{\partial \omega}{\partial A} = 0 \qquad \text{at } \omega = \omega_j \tag{19}$$

The above constraint in conjuction with Eq. (7) leads to

$$\frac{\partial g_2}{\partial A} = \left[\left(1-\omega^2\right)A + F_c\right]\left(1 - \omega^2 + \frac{\partial F_c}{\partial A}\right)$$

$$+ (\omega\zeta A - F_s)(\omega\zeta A - F_s)\left(\omega c - \frac{\partial F_s}{\partial A}\right) = 0 \quad \text{at } \omega = \omega_j \tag{20}$$

Analagous to Eq. (15), we obtain the equation

$$R\omega^4 + S\omega^2 + T = 0 \tag{21}$$

where

$$R = \left(A\frac{\partial F_s}{\partial A} - F_s\right)A^2 \tag{22a}$$

$$S = \left[(\zeta^2 - 2)\left(A\frac{\partial F_s}{\partial A_s} - F_s\right) + 2\left(F_s\frac{\partial F_c}{\partial A} - F_c\frac{\partial F_s}{\partial A}\right)\right]A^2 \tag{22b}$$

$$T = \left[(A - 2F_c)\frac{\partial F_s}{\partial A} - \left(1 + 2\frac{\partial F_c}{\partial A}\right)F_s\right]A^2 - (2AF_s)$$

$$\times\left(F_c\frac{\partial F_c}{\partial A} + F_s\frac{\partial F_s}{\partial A}\right) + (F_s^2 + F_c^2 - 1)\left(F_sA\frac{\partial F_s}{\partial A}\right) \tag{22c}$$

and the frequencies at which jumps occur are obtained by

$$\omega_j = [(-S \pm \sqrt{S^2 - 4RT})/2R]^{1/2} \tag{23}$$

Equation (23) together with Eqs. (6) and (7) provide the basis for calculation of vertical tangencies.

III. Numerical Results

Section III.A shows representative plots of the amplitude as a function of frequency of excitation and discusses how various parameters affect the response. The effects of gap length on dynamic response are shown in Secs. III.B and III.C. Section III.B describes the existence of multiple solutions and how the gap and static preload affect them. The minimum gap length for multiple solutions and how they are affected by preload are discussed in Sec. III.C. Lastly, two cases of transient response are also discussed in Sec. III.C. They show that the system parameters that dictate the steady-state behavior of the system also control transient response.

A. Frequency Response

To examine the validity of the approximate method, Eq. (3) is solved directly using a Runge-Kutta method. The steady-state response is then obtained from the "long-time" transient solution. The results are compared with the ones calculated by the approximate method. These comparisons are plotted in Figs. 3-6 in which the discrete symbols denote the transient solutions and the solid lines represent solutions calculated from Eq. (6) and (7). These figures show that a good agreement exists between the two approaches.

In Fig. 3, the influence of gap length δ on the vibratory amplitude frequency response is shown. For $\delta = 0$, the system is linear. For $\delta \to \infty$, the friction joint is dominated by friction damping, and the friction linkage behaves plastically. In between, a transition region exists for a certain range of δ values where the system shifts from elastic to plastic behavior. In this region, the vibratory amplitude A may become multivalued at some fixed excitation frequencies. A typical case for $\delta = 20$ is shown in the figure.

Multiple solutions also can be seen in Fig. 4, in which amplitudes are calculated for several values of the slip load λ_2. For $\lambda_2 = 2$, the system response is single-valued. Multiple solutions are apparent for $\lambda_2 = 1.0$ and 1.5. For $\lambda_2 = 1.5$, the vibratory amplitude has two disconnected response curves. For $\lambda_2 = 1$, the response curve becomes connected, even though points of vertical tangency may remain at frequencies between 1.035 and 1.04. This implies that for even lower λ_2 values the system response will become single-valued again. The physical explanation of this behavior is that at low λ_2 values, the friction damping has little effect on the system response that is primarily dominated by the constant stiffness k and viscous damping c, and consequently the system behaves nearly linearly. For high λ_2 values, the friction element is partially stuck due to the stronger friction resistance. Under

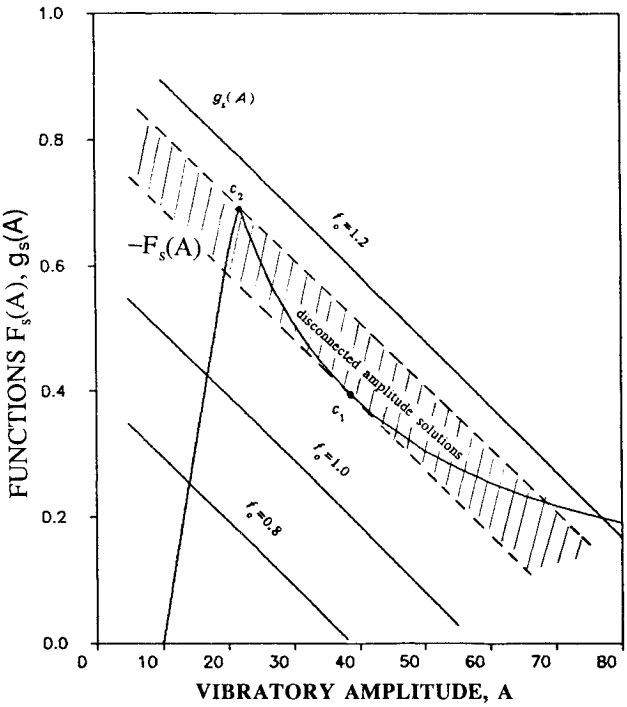

Fig. 7 Resonant vibratory amplitudes as affected by excitation.

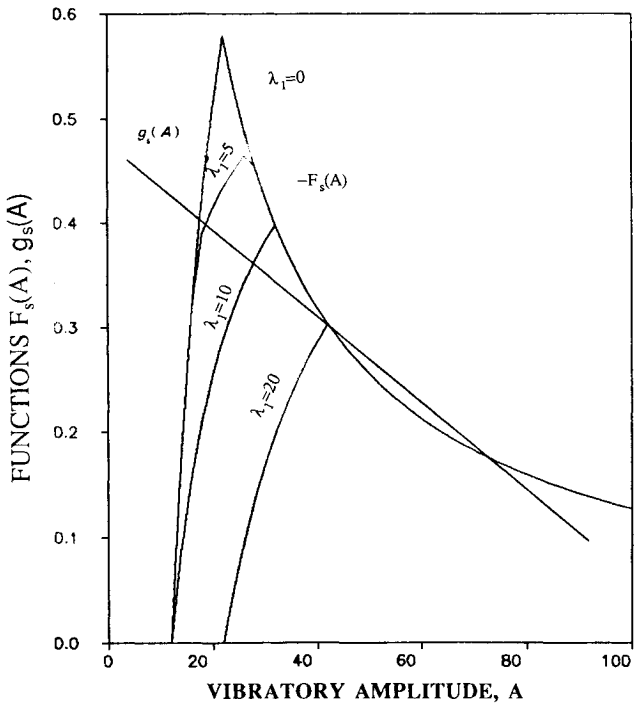

Fig. 8 Effect of static preload on the resonant amplitude response.

this condition, neither of the limit stops is hit during the motion cycle. As a result, the energy dissipation per cycle monotonically increases with amplitude, and the system response is stable. For normal loads in the median range, as the cases of $\lambda_2 = 1.5$ and 1.0 shown in the figure, the limit stops are hit by the element during the motion cycle. Under these conditions, the system response becomes metastable due to the fact that the energy dissipated by friction per cycle cannot increase because of the limit stops, whereas the element stiffness significantly increases with amplitude. This results in the multivalued response indicated in Fig. 4.

Multivalued behavior is also seen in Fig. 5, in which the amplitude is calculated for two stiffness ratios k_d/k. A region having multiple solutions is seen for $k_d/k = 0.25$, where a disconnected closed curve occurs. The appearance of disconnected regions in the more general system model analyzed here agrees well with those observed by Iwan.[13]

The effect of static preload λ_1 on the vibratory amplitude frequency response is shown in Fig. 6. The static preload causes a permanent offset represented by the symbol B, as indicated in Eq. (4). When the system is excited by a large excitation force at the resonant frequency, both limit stops (shown in Fig. 2) are hit during the motion cycle, and the offset has little effect on the vibratory amplitude. However, at some off-resonant frequencies, the response is sufficiently low that there is a difference in the response. Without the static preload, the limit stops would not be encountered during the motion cycle. However, once the static load is applied, the permanent offset thus generated adds to the dynamic displacement and causes the friction element to hit one of the stops and reduces damping in the system. Consequently, the vibratory amplitude increases at off-resonant frequencies as illustrated in the figure. For low excitation force, the static load may even raise the maximum amplitude of the system.

Thus, it is seen that under certain conditions static preload can have a significant effect on vibratory response. For some excitation, the presence of a large static load may even eliminate the multivalued response and stabilize the system. This means that gravitational effects may strongly affect the dynamic response of structures that are ground tested and their behavior might be quite different from the actual response that would occur in space. Therefore, this effect needs to be carefully analyzed in order to interpret laboratory test data properly so as to predict the response of the full-scale structure in space.

B. Effect of Gap Length on the Existence of Multiple Solutions

In this section, we establish a procedure for calculating the range of gap lengths for which multiple, disconnected solutions exist. We do this by reconsidering the equations for maximum response given in Eqs. (18). The presence of multiple solutions is primarily due to the nature of Eq. (18b). This can be seen by using the following ploy. First, rearrange Eq. (18b) into the following form:

$$-F_s(A,B) = g_s(A,\omega_m) \equiv \frac{1}{\sqrt{1+(\zeta/2\omega_m)^2}} - \omega_m \zeta A \qquad (24)$$

which says that, at resonance, $-F_s$ is equal to the function g_s as defined in Eq. (24). In addition, at resonance, A, B, and ω_m must satisfy Eqs. (18a) and (18c). From Eq. (18a), B can be calculated as an implicit function of A and from Eq. (18c), ω_m can be determined as an implicit function of A. From Ref. 18, the specific functional form of F_s can be written, and by using $B(A)$ we can plot F_s as a function of A alone that satisfies both Eqs. (18a) and (18c), i.e., $F_s(A) = F_s[A,B(A)]$. Similarly, from Eq. (24) we can plot $g_s(A) = g_s(A) = g_s[A, \omega_m(A)]$ that satisfies Eqs. (18a) and (18c). Then from Eq. (24) we know that Eqs. (18a–18c) are satisfied and that we have resonance at points where the two functions intersect. Plots of the functions are shown in Figs. 7 and 8 for a range of values of f_o and λ_1, respectively. (In these figures, we use the dimensional parameters f_o and $\bar{A}$ so as to more easily discuss the role of excitation on the response $\bar{A} = A \cdot f_o/k$.)

It is now apparent under what conditions multiple solutions occur. The function g_s is almost a linear function of $\bar{A}$ because the resonant frequency is nearly constant (approximately 1.0). In Fig. 7, it is clear that for different excitation levels, an unstable region of two disconnected amplitude-response curves exists between points c1 and c2. This is indicated by the three resonant amplitudes shown in the figure: the upper two values are the maximum and minimum amplitudes of the upper closed-response curve, whereas the lowest one is

the maximum amplitude of the lower response curve. Physically, point c1 indicates the maximum excitation for which the stable response is obtained. In this situation, usually only one of the limit stops is encountered by the friction element during the motion cycle. This indicates that for constant excitation f_o a critical gap length δ_{cr} exists beyond which the response remains unchanged. With this understanding of the process, δ_{cr} can be obtained by the geometric requirement at point c1 that the slopes of the curves as well as their values are equal, i.e.,

$$\frac{\partial F_s}{\partial \bar{A}} = -\frac{\partial g_s}{\partial \bar{A}} = \omega c, \qquad -F_s = g_s \tag{25}$$

when B is constant.

Point c2 indicates the maximum excitation for disconnected solutions to appear. Alternatively, for constant excitation f_o, this point denotes the minimum gap length δ_m for which the system has disconnected amplitude solutions. It can be inferred that the point c2 is where the friction element touches both of the stops at the lower resonant amplitude. Therefore, the gap length δ_m can be determined from the equation

$$\delta_m = 2\left(\bar{A}_\infty - \frac{\mu N}{k_d}\right) \tag{26}$$

where $\bar{A}_\infty$ = the resonant amplitude at $\delta = \infty$.

The effect of static preload on the region where the disconnected solutions occur is depicted in Fig. 8. It is apparent that the static load tends to play an on/off role on this region. When this load is below a certain value, only the lowest resonant amplitude is affected and the response remains disconnected. Once this load is raised above a critical value (20 in the case shown), the amplitude solutions become single valued.

C. Minimum Gap Length for Vertical Jumps

As was discussed in the last section, disconnected solutions exist between limit gaps δ_{cr} and δ_m. For gap length less than δ_m, the system response becomes connected; however, multiple solutions may still exist corresponding to connected response curves of the type depicted for $\delta = 20$ in Fig. 3. Thus, multiple solutions can occur until the gap is further reduced below a limit δ_j.

The response depicted in Fig. 9 may be used to illustrate this argument. The locus of vertical tangencies is presented in broken lines that define a closed region. In this plot, the excitation f_o is varied while the gap is kept constant. The intersections of the response curves and the locus indicate where individual vertical tangencies occur. In the figure, it is clear that vertical tangencies only occur when the limit stops are hit during the motion cycle. They disappear when the excitation f_o is large enough that the response curve passes beyond point a_1 or a_2 (whichever is crossed secondly). At constant excitation, we may define a limit gap δ_j. If δ is less than δ_j, then the solution is single-valued. Its value can be obtained by calculating under what conditions the response curve intersects the locus at either point a_1 or a_2 (whichever leads to the smaller δ_j). The choice between points a_1 or a_2 as the crossing point is affected by the stiffness k_d/k. When the stiffness k_d/k is large, the response curve is more slanted to the left and point a_2 will be passed by first as the gap length is reduced. The point a_1 is then the intersection used to determine the limit gap δ_j, and vice versa.

In Fig. 10, the effect of static preload on the jump locus is depicted. It is seen that the closed region of the jump locus shrinks as the load is increased. At the same time, the jump limit gap δ_j is raised in value.

The limit gaps δ_{cr}, δ_m, and δ_j as functions of the slip load λ_2 are shown in Fig. 11. As shown in the plot, three regions exist. When the slip load approaches zero, regions II and III shrink, and all the limit gaps δ_{cr}, δ_m, and δ_j tend to infinity. The system response then becomes linear. At a large scale value of $\lambda 2$, limit-gap curves δ_{cr} and δ_m coincide, and the disconnected response (region II) disappears. However, the region of connected, multiple solutions (region III) remains until λ_2 reaches a sufficiently large value so that the friction element becomes stuck and the gap no longer affects the response.

D. Effects on the Transient Solutions

One reason for studying the system's steady-state behavior is to gain a better understanding of its transient response. We have been examining conditions under which the steady-state response may exhibit multiple solutions. These conditions also

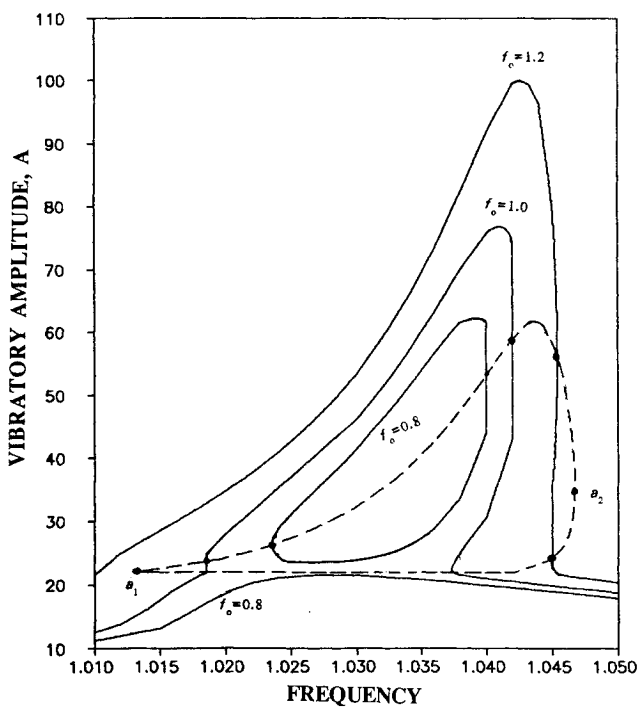

Fig. 9 Locus of vertical tangencies in the frequency domain.

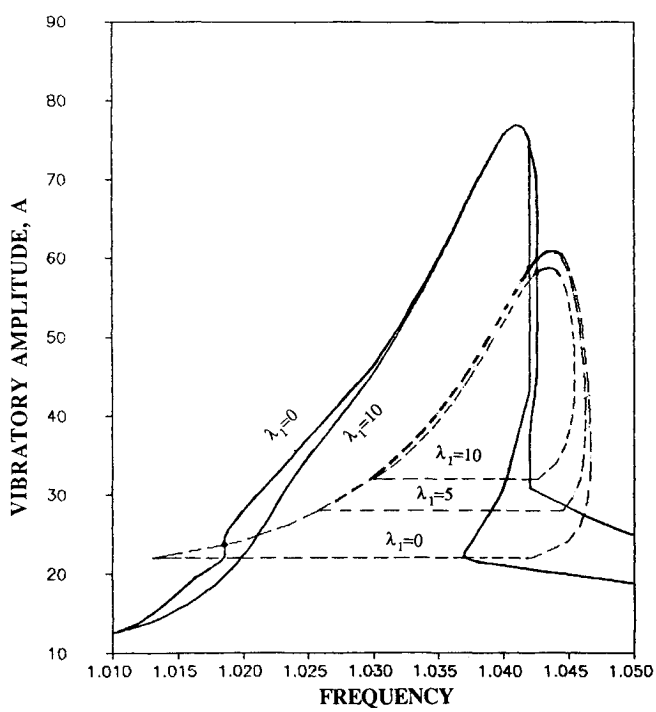

Fig. 10 Locus of vertical tangencies as affected by the static load.

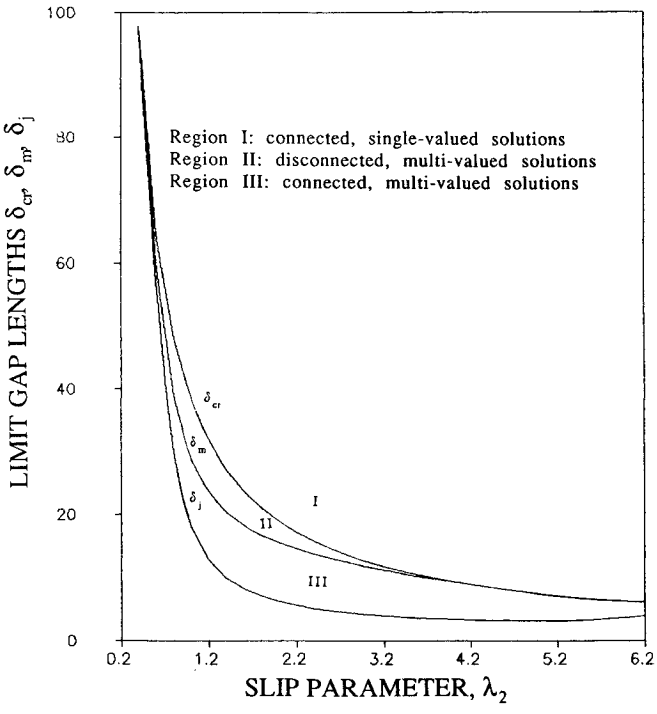

Fig. 11 Limit gap curves as affected by the normal load.

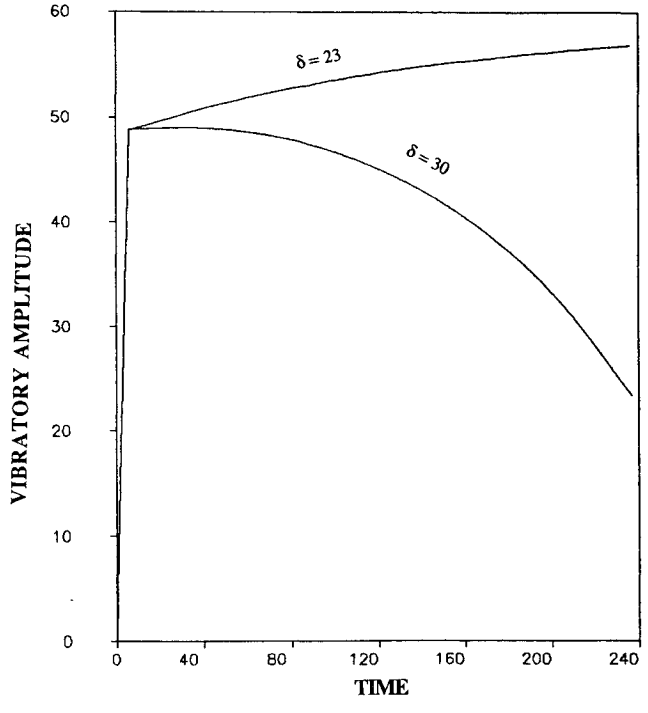

Fig. 12 Effect of gap length on the transient response.

affect transient response. For example, when the system parameters are such that it has multiple solutions, then altering slightly one of the parameters can lead to quite different transient response.

In Fig. 12, the amplitudes of two systems are plotted as functions of time. One case corresponds to $\delta = 23$ and the other to $\delta = 30$. For short times the responses are identical. However, for longer times they differ radically. It is known from the previous sections that, for conditions corresponding to multiple solutions, different initial conditions may lead to different vibratory amplitude at the steady state. In the previous section, we showed that the gap length also affects the presence of multiple solutions. Consequently, even for the

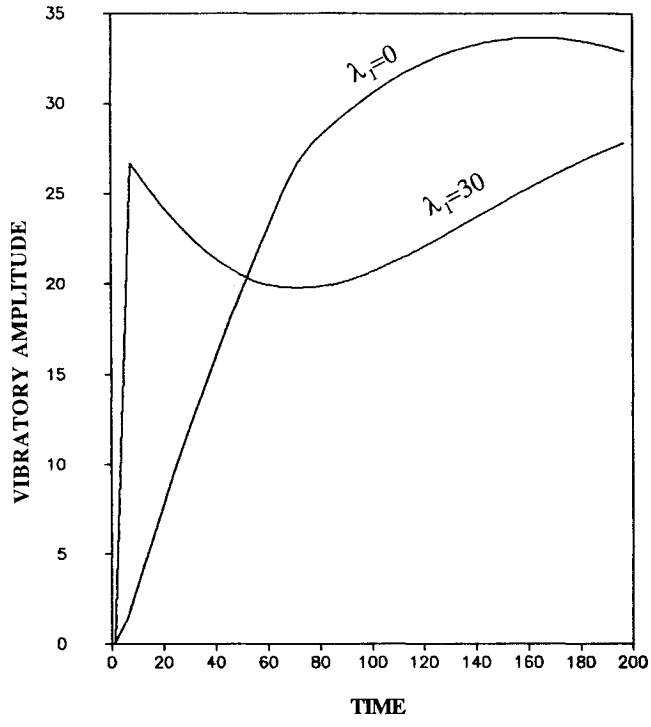

Fig. 13 Effect of static load on the transient respone.

same initial conditions, changes in the gap length can lead to quite different transient responses.

The effect of static preload is illustrated in Fig. 13. In this case, the preload accentuates the response for short times and attentuates it later.

These results relate to the ground testing of scale models of large space structures. They indicate that a larger gap may reduce the amplitude of response, whereas an applied static load may produce an opposite effect. Compared to the full-scale structure, the scale model tends to have larger joint tolerances relative to its smaller overall size. In addition, a large static preload (due to gravity) may be present during ground testing. Since these two factors sometimes contribute opposite effects, they have an unknown qualitative and quantitative effect on the test results. This indicates the need for a careful analysis of the experimental data in order to predict properly the response of the full-scale structure in space.

IV. Conclusions

It has been found that under certain conditions the vibratory amplitude of the system may become multivalued over a range of excitation frequencies. A large jointed structure may have significant variations in the joint properties from joint to joint due to machining differences. As a result, some of the joints may experience the conditions that lead to multivalue response. Consequently, it may be difficult to get repeatable experimental results since the structure may settle into different patterns of response depending on fairly subtle aspects of how the loads are applied. The difficulty is intensified for laboratory tests of scaled models of space structures since the scatter in the joint's free play is relatively larger with respect to the smaller dimensions of the model joint.

This work also shows that under some conditions the presence of static preloads may affect significantly the system's dynamic response. In this case, if a large structure is ground tested, it may be necessary to first correlate the data with an analytic model of the structure that includes preload effects, and then eliminate the preloads in the model and predict its behavior in space.

Lastly, it should be noted that our results suggest that if the space structure is more flexible, it may, in fact, have less problems. This is because if the structure is flexible, then k_s in

Fig. 1 is small and, as a result, one can observe from Eq. (1) that k_d/k tends to be small. From Fig. 5, it is clear that reducing k_d/k reduces the strength of the nonlinearity and tends to make the system respond in a single-valued manner. To what extent this would actually alleviate the problems we have discussed would depend on the specific attributes of the system under consideration.

Acknowledgments

This work was supported by NASA Langley Research Center, Grant NAG-1-612-NA64, under the direction of Mr. Lucas Horta. We also express our appreciation to the referees for their helpful comments.

References

[1]Hertz, T. J. and Crawley, E. F., "Damping in Space Structure Joints," *Proceedings of the AIAA Dynamics Specialists Conference*, May 1984, AIAA, New York.

[2]Pian, T. H H., "Structural Damping of Simple Built-Up Beam with Riveted Joint in Bending," *ASME Journal of Applied Mechanics*, Vol. 24, March 1957, pp. 33-35.

[3]Menq, C.-H., Bielak, J., and Griffin, J. H., "The Influence of Microslip on Vibratory Response, Part 1: A New Theoretical Model,' *Journal of Sound and Vibration*, Vol. 107, June 1986, pp. 279-293.

[4]Meng, C-H., Griffin, J. H., and Bielak, J., "The Influence of Microslip on Vibratory Response, Part 2: A Comparison with Experimental Results," *Journal of Sound and Vibration*, Vol. 107, June 1986, pp. 295-307.

[5]Den Hartog, J. P., *Mechanical Vibrations*, 4th ed. McGraw-Hill, Chapter 8, New York, 1956.

[6]Hanks, B. R. and Pinson, L. D., "Large Space Structures Raise Testing Chanllenges," *Astronautics and Aeronautics*, Vol. 21, No. 10, 1983, p. 34-40, 53.

[7]Crawley, E. F. and Aubert, A. C., "Identification of Nonlinear Structural Elements by Force-State Mapping," *AIAA Journal*, Vol. 24, Jan. 1986, pp. 155-162.

[8]Plunkett, R., "Friction Damping," *Damping Applications for Vibration Control*, American Society of Mechanical Engineers, ASME Booklet AMD-Vol. 38, New York, 1980.

[9]Jones, D. I. G., "High-Temperature Damping of Dynamic Systems," *Shock Vibration Digest*, Vol. 17, No. 10, 1985, pp. 3-5.

[10]Beards, C. F., "Damping in Structural Joints," *Shock Vibration Digest*, Vol. 17, No. 11, 1985, pp. 17-20.

[11]Den Hartog, J. P., "Force Vibrations with Combined Coulomb and Viscous Friction," *Transactions of the ASME*, APM-53-9, 1931, pp. 107-115.

[12]Caughey, T. K., "Sinusoidal Excitation of a System with Bilinear Hysteresis," *ASME Journal of Applied Mechanics*, Vol. 27, Dec. 1960, pp. 640-643.

[13]Iwan, W. D., "Steady-State Dynamic Respone of a Limit Slip System," *ASME Journal of Applied Mechanics*, Vol. 35, June, 1968, pp. 322-326.

[14]Nayfeh, A. H and Mook, D. T., *Nonlinear Oscillations*, Wiley, New York, 1979.

[15]Gelb, A. and Vander Velde, W. E., *Multiple-Input Describing Functions and Nonlinear System Design*, McGraw-Hill, New York, 1968.

[16]Iwan, W. D., "Application of Nonlinear Analysis Techniques," *Applied Mechanics in Earthquake Engineering*, edited by W. D. Iwan, ASME Applied Mechanics Division Publication Vol. 8, 1974.

[17]Menq, C.-H., Griffin, J. H., and Bielak, J., "The Influence of a Variable Normal Load on the Force Vibration on the Forced Vibration of a Frictionally Dampled Structured," *ASME Journal of Engineering for Gas Turbines and Power*, Vol. 108, No. 2, April 1986, pp. 300-305.

[18]Hsu, S. T., Griffin, J. H., and Bielak, J., "How Gravity and Joint Scaling Affect Structural Response," Dept. of Mechanical Engineering, Carnegie Mellon Univ., Pittsburgh, PA, SM Rept. 88-7, Aug. 1988.

Recommended Reading from the AIAA Progress in Astronautics and Aeronautics Series . . .

Single- and Multi-Phase Flows in an Electromagnetic Field: Energy, Metallurgical and Solar Applications

Herman Branover, Paul S. Lykoudis, and Michael Mond, editors

This text deals with experimental aspects of simple and multi-phase flows applied to power-generation devices. It treats laminar and turbulent flow, two-phase flows in the presence of magnetic fields, MHD power generation, with special attention to solar liquid-metal MHD power generation, MHD problems in fission and fusion reactors, and metallurgical applications. Unique in its interface of theory and practice, the book will particularly aid engineers in power production, nuclear systems, and metallurgical applications. Extensive references supplement the text.

TO ORDER: Write AIAA Order Department,
370 L'Enfant Promenade, S.W., Washington, DC 20024
Please include postage and handling fee of $4.50 with all orders. California and D.C. residents must add 6% sales tax. All foreign orders must be prepaid.

1985 762 pp., illus. Hardback
ISBN 0-930403-04-5
AIAA Members $59.95
Nonmembers $89.95
Order Number V-100